

# DIELECTRIC RESPONSE OF THICK LOW DISLOCATION-DENSITY Ge EPILAYERS GROWN ON (001) Si

Kelly E. Junge, Rüdiger Lange, Jennifer M. Dolan, and Stefan Zollner  
Ames Laboratory and Department of Physics and Astronomy,  
Iowa State University, Ames, IA 50011

M. Dashiell, B.A. Orner, and J. Kolodzey  
Department of Electrical and Computer Engineering,  
140 Evans Hall, University of Delaware, Newark, DE 19716

## ABSTRACT

Spectroscopic ellipsometry was used to measure the dielectric functions of epitaxial and bulk Ge at photon energies from 1.5 to 5.2 eV. The epitaxial Ge was grown at 400°C by molecular beam epitaxy on (001) Si substrates. The optical response and the interband critical-point parameters of Ge on Si were found to be indistinguishable from that of bulk single crystal Ge, indicating high optical quality. Dislocation density measurements using an iodine etch verified low surface defect densities. We conclude that epitaxial Ge grown on Si at relatively low temperatures is suitable for optical device applications.

## INTRODUCTION

Because of the large lattice mismatch ( $\sim 4\%$ ) between Si and Ge and their different thermal expansion coefficients, it is difficult to produce high-quality heteroepitaxial Ge films on Si substrates. On the other hand, the growth of low defect-density Ge [1,2] and  $\text{Si}_{1-x-y}\text{Ge}_x\text{C}_y$  alloys [3-5] on Si (001) is of great technological interest to modify transport [3,4,6] and carrier confinement in Si-based devices and to integrate Ge-based optoelectronics (e.g., infrared detectors) with well-developed Si integrated circuit technology. Also, because of the small lattice mismatch of GaAs and Ge, it becomes feasible to integrate III/V devices with Si VLSI technology by growing a Ge virtual substrate on Si, followed by GaAs/Ge epilayers [7].

The initial growth of Ge on Si (001) can be described [8] as Stranski-Krastanow: The first three to six monolayers grow layer-by-layer. After about 10 to 15 Å, islands start to form. Island formation can be suppressed by a surfactant (As), extending the layer-by-layer growth [8]. Because of the local elastic deformation of near-surface layers in the substrate, the onset of dislocations is delayed [8] until the islands have grown to far in excess (500 Å) of the equilibrium critical thickness (10 Å).

This work deals with much thicker layers, where the strain is relieved by misfit dislocations. These dislocations can be studied using plan-view transmission electron microscopy (TEM) [2,4,9]. They usually climb to the surface where they deteriorate the transport properties of active device layers (such as a heterojunction bipolar transistor [4]). Using thick compositionally graded layers [10], it is possible to grow relaxed  $\text{Si}_{1-x}\text{Ge}_x$  layers ( $x \sim 0.3$ ) with low threading dislocation densities.

Malta *et al.* [2] have shown that dislocations in Ge on Si can be confined to the epilayer/substrate interface (extending up to 0.7  $\mu\text{m}$  from the interface) by growing with

substrate temperatures near the melting point of Ge (937°C). For samples with a thickness of 2.5  $\mu\text{m}$ , the residual strain was  $\epsilon \sim 2.5 \times 10^{-3}$  and the etch pit density, a measure for the dislocation density at the surface, was about  $2 \times 10^5 \text{ cm}^{-2}$ . Apparently, interfacial Ge melts and subsequently alloys with the Si substrate. Growth at intermediate temperatures (700°C) does not confine the dislocations, resulting in a higher etch pit density.

The purpose of this work is to show that slow growth at low temperatures can yield thick Ge films on Si with low surface dislocation densities. This leads to the surprising result that the dielectric function of Ge on Si is indistinguishable from that of a bulk Ge sample. (The correlation between the dielectric function and of dislocations in group-IV alloys was discussed by Lange *et al.* [11].)

## GROWTH

The Ge layers used in this study were grown by molecular beam epitaxy (MBE) in an EPI-620 system [12] having a base pressure less than  $5 \times 10^{-11}$  Torr. The Ge molecular beam was produced by thermal evaporation from a solid source of zone-refined polycrystalline Ge in a pyrolytic boron nitride crucible. To minimize contamination from the crucible, the cell temperature was kept below 1380°C. At the cell temperature of 1325°C used in this experiment, the Ge growth rate was 0.11  $\mu\text{m}/\text{hour}$  (0.3  $\text{\AA}/\text{s}$ ).

Substrates were (001) oriented, 75 mm diameter silicon wafers prepared by degreasing, oxidizing in a solution of  $\text{H}_2\text{O}:\text{H}_2\text{O}_2:\text{HCl}$  (5:3:3), and dipping in  $\text{HF}:\text{H}_2\text{O}$  (1:10) [12]. The substrates were desorbed at 250°C in the MBE chamber just prior to growth. The Ge layers were grown at a substrate temperature of 400°C; they were between 0.3 and 1.1  $\mu\text{m}$  thick (measured by a Dektak) and appeared mirror-smooth after growth. Since the mobility of dislocations is limited at lower temperatures [9] and the thermal expansion coefficient of Ge ( $6 \times 10^{-6}$ ) is about a factor of two larger than that of Si, it is not surprising that growth at low temperatures resulted in high quality layers.

## CHARACTERIZATION

### Reflection High-Energy Electron Diffraction

Well resolved reciprocal lattice rods of the substrate were observed by *in situ* reflection high energy electron diffraction (RHEED). After about 10  $\text{\AA}$  of growth, the lattice rods were less well resolved, but distinct rods still remained. The RHEED pattern gradually improved as the epilayer became thicker. For sample SGC99, a 0.75  $\mu\text{m}$  thick layer of Ge on Si grown at 400°C, the RHEED pattern at the completion of growth was similar in features and intensity to that of commercially available Ge substrates. The RHEED suggested that island formation was partially suppressed at low growth temperatures, and that as growth proceeds islands may coalesce to form single crystal Ge with few defects. We speculate that the low growth rates employed here encourage the formation of reduced defect single crystal Ge over multicrystalline Ge, but further study will be necessary to confirm this.

### Etch Pit and Dislocation Densities

To find the surface dislocation densities, we used an iodine etch [2]  $\text{HF}:\text{HNO}_3:\text{CH}_3\text{COOH}:\text{I}$  (20 ml:40 ml:44 ml:120 mg) for 1 s to measure the etch pit density of the Ge layers. For

SGC99, it appeared constant and uniform across the entire area and was consistent between samples and etch times. The average etch pit density was  $4 \times 10^4 \text{ cm}^{-2}$ , a factor of five lower than the results of Malta *et al.* [2]. The etch pit densities of thinner layers ( $< 0.3 \text{ }\mu\text{m}$ ) and those of samples grown at higher temperatures ( $> 500 \text{ }^\circ\text{C}$ ) could not be determined, since the etch pit density was not uniform or the complete Ge layer was removed by the etch. The etch pit density of bulk Ge was less than  $10^4 \text{ cm}^{-2}$ , consistent with data supplied by Eagle Picher. The pit shapes for SGC99 and bulk Ge differed. For the bulk Ge, most pits were circular, about  $1 \text{ }\mu\text{m}$  in diameter. For SGC99, the pits were squares, approximately  $1\text{--}3 \text{ }\mu\text{m}$  on each side.

### Dielectric Function

After growth, the dielectric functions  $\epsilon$  in the 1.5 to 5.5 eV photon-energy range were measured *ex situ* with a spectroscopic ellipsometer [13]. The spectra were corrected for a native oxide layer. The thickness of the oxide was determined by matching  $\epsilon_2$  at its peak near 4.2 eV with the data of Ref. [13]. The lines in Fig. 1 show the real ( $\epsilon_1$ ) and imaginary ( $\epsilon_2$ ) parts of  $\epsilon$  for sample SGC99, assuming an oxide thickness of  $10 \text{ }\text{\AA}$ . Other Ge epilayers grown on Si at the same temperature (not shown in the figure) had similar  $\epsilon$ . For comparison, we also measured  $\epsilon$  for a commercial bulk Ge  $\langle 001 \rangle$  sample (Eagle Picher). The dielectric function of SGC99 and that of the bulk sample were indistinguishable, except below 1.8 eV, where the accuracy of our instrument decreases. In Fig. 1 we also show the data of Ref. [13] ( $\bullet$ ,  $\triangle$ ) for bulk  $\langle 111 \rangle$  Ge. The agreement is good, except for  $\epsilon_2$  in the range below 2 eV. (Similar discrepancies were found in Ref. [16].) The dielectric function of SGC99 resembles that of bulk Ge much more than that of thin Ge films enclosed between Si barriers [14, 15].

### Critical-Point Analysis

The spectra show a double-peak structure above 2 eV ( $E_1$ ,  $E_1 + \Delta_1$ ), a shoulder near 3 eV ( $E'_0$ ) and a third peak near 4.2 eV ( $E_2$ ). These peaks are interband critical points (CPs) arising from direct band-to-band transitions at various regions in the Brillouin zone [17]. For a further analysis of these CPs, we calculate numerically the second derivative of  $\epsilon$  with respect to photon energy (shown by the symbols in Fig. 2) and perform a line shape analysis. Following Viña *et al.* [17], we describe the CPs using a mixture of a 2-D minimum and a saddle point represented by

$$\epsilon(\omega) = C - A \ln(\hbar\omega - E_g - i\Gamma) \exp(i\phi), \quad (1)$$

where  $\hbar\omega$  is the photon energy,  $E_g$  the energy of the CP,  $\Gamma$  its broadening,  $A$  its amplitude (oscillator strength), and  $\phi$  the phase angle describing the amount of mixing. The parameters obtained from the line shape analysis are given in Table 1 in comparison with parameters of bulk samples from Viña and coworkers [17]. First, we note that our bulk parameters are, within the error bars, identical to those of Ref. [17] with one exception: Viña and coworkers used a fixed spin-orbit splitting  $\Delta_1 = 187 \text{ meV}$  determined from low-temperature measurements. In our analysis, we treated  $\Delta_1$  as a free parameter (since it is a measure for the strain in the sample) and found  $\Delta_1 = 200 \text{ meV}$  for bulk Ge.

The CP parameters for sample SGC99 are similar to those of bulk Ge. Most importantly, the broadenings, related to defects, are essentially the same. Therefore, the scattering

dielectric function  $\epsilon$

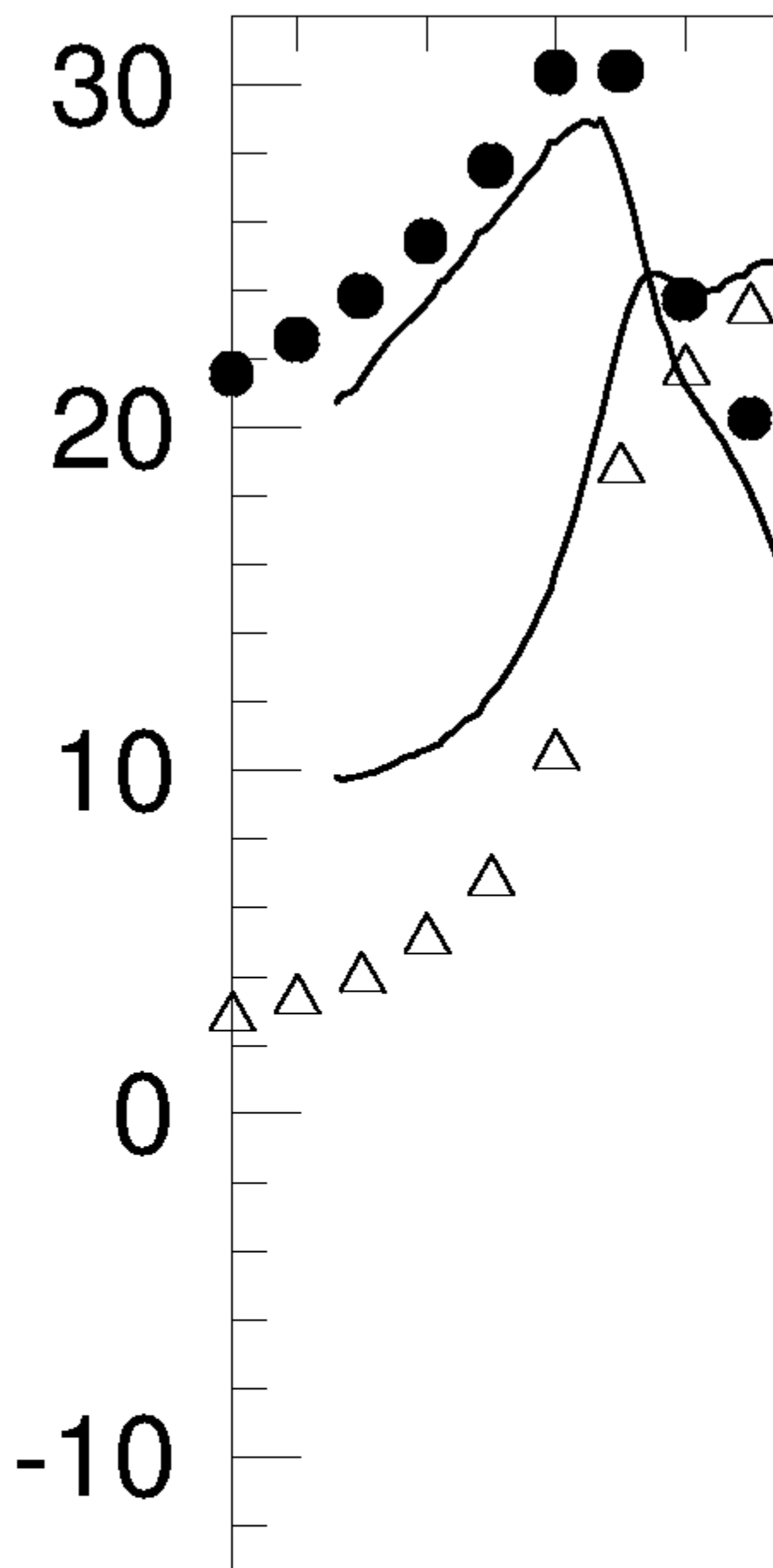


Table 1: Critical point (CP) parameters for bulk Ge and Ge on Si: amplitude ( $A$ ), energy ( $E$ ), broadening ( $\Gamma$ ), and excitonic phase ( $\Phi$ ), see Eq. (1).

	$A$ (1)	$E$ (eV)	$\Gamma$ (eV)	$\Phi$ (deg)
Bulk Ge (this work)				
$E_1$	5.5(3)	2.114(2)	0.058(2)	86(4)
$E_1 + \Delta_1$	4.1(6)	2.314(2)	0.076(6)	same
$E'_0$	3.2(6)	3.05(2)	0.20(2)	-29(12)
$E_2$	8(1)	4.37(1)	0.107(1)	-193(11)
Bulk Ge (from Ref. [17])				
$E_1$		2.111(3)	0.06(1)	71(4)
$E_1 + \Delta_1$		2.298(3)	0.07(2)	same
$E'_0$		3.11		
$E_2$		4.368(4)	0.109(9)	
Ge on Si (SGC99, this work)				
$E_1$	6.2(4)	2.116(2)	0.063(2)	84(4)
$E_1 + \Delta_1$	3.7(7)	2.322(2)	0.076(6)	same
$E'_0$	3.3(5)	3.05(2)	0.21(2)	-29(9)
$E_2$	8(1)	4.37(1)	0.109(6)	-196(6)

## CONCLUSION

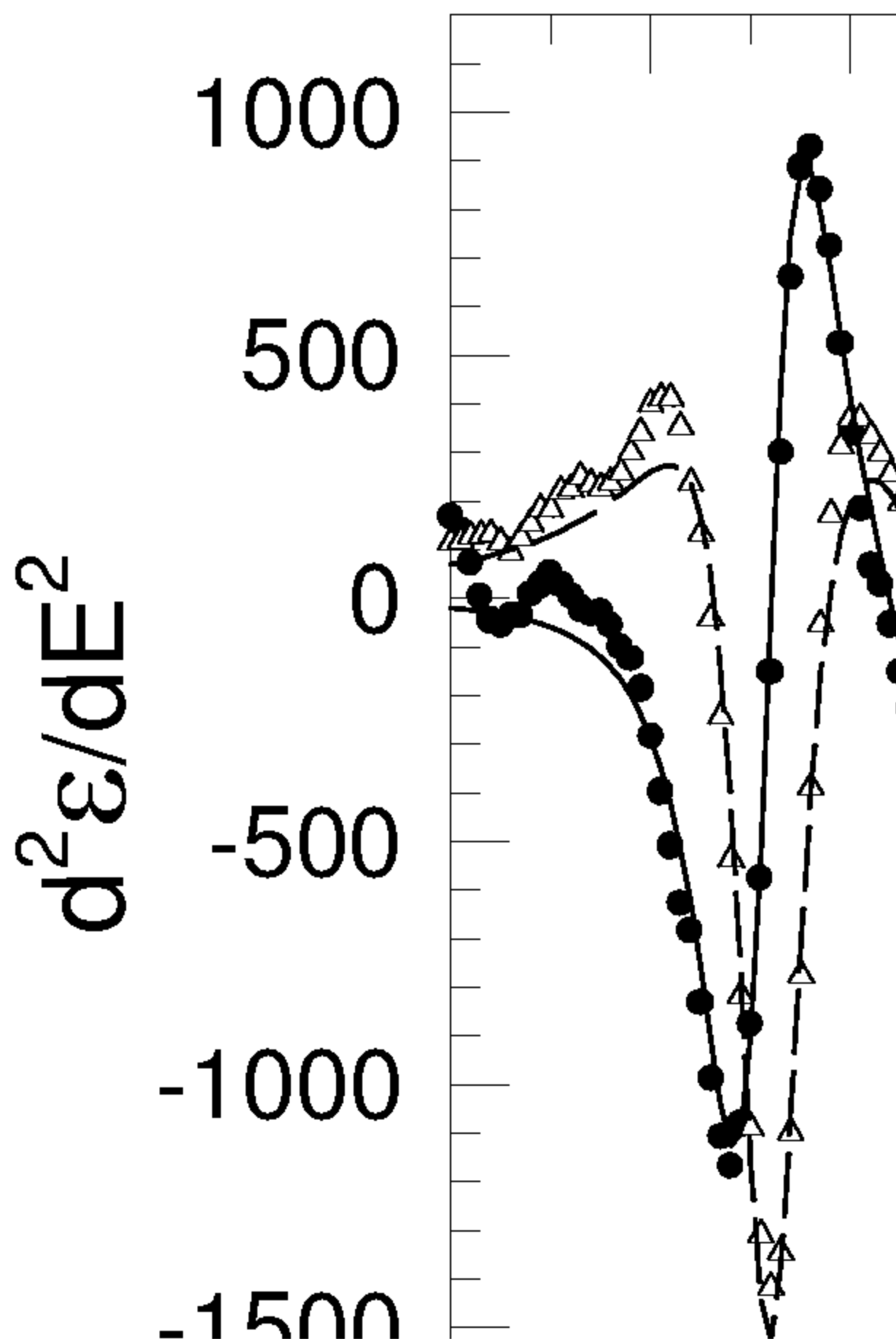
In conclusion, we have found that the optical constants (refractive index and absorption coefficient) and their derivatives, related to band structure and transport parameters (CP energies and broadenings), of thick Ge layers on Si are virtually identical to those of bulk Ge. These results are in agreement with RHEED and EPD counts. Therefore, we should expect that electronic and optoelectronic devices fabricated using Ge on Si should have similar (if not superior) characteristics compared to bulk Ge-based devices.

## ACKNOWLEDGEMENTS

Ames Laboratory is operated for the U.S. Department of Energy by Iowa State University under Contract No. W-7405-Eng-82. The work at Ames was supported by the Iowa Space Grant Consortium, the Director of Energy Research, Office of Basic Energy Sciences, and by the National Science Foundation (DMR-9413492). The work at Delaware was supported by the Air Force Office of Scientific Research (F49620-95-0135), the Army Research Office (DAAH04-95-1-0625), DARPA, and the Office of Naval Research (N00014-93-1-0393).

## REFERENCES

- [1] B.-Y. Tsaur, M.W. Geis, J.C.C. Fan, and R.P. Gale, Appl. Phys. Lett. **38**, 779 (1981); J.M. Baribeau, T.E. Jackman, D.C. Houghton, P. Maingé, and M.W. Denhoff, J. Appl.



- [11] R. Lange, K.E. Junge, S. Zollner, S.S. Iyer, A.P. Powell, and K. Eberl, J. Appl. Phys. (Oct. 15, 1996).
- [12] J. Kolodzey, P.A. O'Neil, S. Zhang, B.A. Orner, K. Roe, K.M. Unruh, C.P. Swann, M.M. Waite, and S. Ismat Shah, Appl. Phys. Lett. **67**, 1865 (1995).
- [13] D.E. Aspnes and A.A. Studna, Phys. Rev. B **27**, 985 (1983).
- [14] J.L. Freeouf, J.C. Tsang, F.K. LeGoues, and S.S. Iyer, Phys. Rev. Lett. **64**, 315 (1990).
- [15] J.E. Hulse and S.J. Rolfe, Thin Solid Films **93**, 223 (1993).
- [16] P. Etchegoin, J. Kircher, M. Cardona, and C. Grein, Phys. Rev. B **45**, 11721 (1992).
- [17] L. Viña, S. Logothetidis, and M. Cardona, Phys. Rev. B **30**, 1979 (1984).